

Article

Spectroscopy and Microscopy of Corundum from Primary Deposits Found in Greece

Vilemini Karantoni ¹, Stefanos Karampelas ², Panagiotis Voudouris ^{3,*}, Vasilios Melfos ^{1,*},
Lambrini Papadopoulou ¹, Triantafyllos Soldatos ¹ and Constantinos Mavrogonatos ³

¹ School of Geology, Aristotle University of Thessaloniki, 54124 Thessaloniki, Greece; vileminikar@gmail.com (V.K.); lambrini@geo.auth.gr (L.P.); soldatos@geo.auth.gr (T.S.)

² Laboratoire Français de Gemmologie, 30 rue de la Victoire, 75009 Paris, France; s.karampelas@lfg.paris

³ Faculty of Geology and Geoenvironment, National and Kapodistrian University of Athens, 15784 Athens, Greece; kmavrogon@geol.uoa.gr

* Correspondence: voudouris@geol.uoa.gr (P.V.); melfosv@geo.auth.gr (V.M.); Tel.: +30-210-7274129 (P.V.); +30-2310-998539 (V.M.)

Abstract: Corundum primary deposits in Greece occur in four locations: Paranesti in Drama and Gorgona in Xanthi, both belonging to the wider Rhodope Massif, as well as, Ikaria island and Kinidaros in Naxos island, both belonging to Attic-Cycladic Massif. Eight samples were examined with spectroscopic methods (FTIR, UV-Vis, EDXRF) in order to better characterize these four primary deposits: two pink sapphires from Paranesti, a pink and a blue sapphire from Gorgona, two blue sapphires from Ikaria and three blue sapphires from Kinidaros. Under the microscope, all samples present characteristics linked to post-crystallization deformation, decreasing their gem quality. The FTIR absorption spectra of all samples present in different relative intensities, bands of boehmite, diaspore, goethite, mica and/or chlorite inclusions and CO₂ in fluid inclusions. Boehmite and diaspore inclusions are most likely epigenetic. In the UV-Vis spectra, the pink color of the samples is linked with Cr³⁺ absorptions and the blue color with absorptions due to Fe²⁺-Ti⁴⁺ intervalence charge transfer. EDXRF analyses in the studied samples show relatively high titanium and iron concentrations that are related with mineral inclusions. Gallium is slightly variable in samples from different regions; also, different colored samples from Gorgona present diverse gallium content.

Keywords: corundum; sapphire; Greece; FTIR; UV-Vis; EDXRF



Citation: Karantoni, V.; Karampelas, S.; Voudouris, P.; Melfos, V.; Papadopoulou, L.; Soldatos, T.; Mavrogonatos, C. Spectroscopy and Microscopy of Corundum from Primary Deposits Found in Greece. *Minerals* **2021**, *11*, 750. <https://doi.org/10.3390/min11070750>

Academic Editors: Franca Caucia and Luigi Marinoni

Received: 24 April 2021

Accepted: 7 July 2021

Published: 10 July 2021

Publisher's Note: MDPI stays neutral with regard to jurisdictional claims in published maps and institutional affiliations.



Copyright: © 2021 by the authors. Licensee MDPI, Basel, Switzerland. This article is an open access article distributed under the terms and conditions of the Creative Commons Attribution (CC BY) license (<https://creativecommons.org/licenses/by/4.0/>).

1. Introduction

Corundum (Al₂O₃) is an allochromatic mineral; “ruby” is referred to its red color variety, “sapphire” is the blue variety, while any other colored corundum is called fancy sapphire and requires the color prefix (e.g., pink sapphire, purple sapphire, colorless sapphire). The colors of corundum are principally related to four elements Cr, Fe, Ti, and V [1–3]. Most gem-quality sapphires and some rubies are found in secondary placer deposits worldwide, and little is known about their crystallization conditions in their geological environment [4–19].

Corundum is rarely found in Greece. Four primary occurrences of corundum are discovered in Greece (Figure 1), two at the Rhodope massif (Paranesti in Drama and Gorgona at Xanthi) and two at the Attic-Cycladic massif (Ikaria island and Kinidaros in Naxos island). These two geotectonic units represent major metamorphic core complexes that were exhumed along large detachment fault systems during the Cenozoic. Previous studies have focused on mineralogical, petrographic, geochemical, isotopic and fluid inclusions studies for the determination of the geological environment of the formation of the Greek corundum [20–27].

The rubies and pink sapphires occur at Paranesti in Drama within boudinaged amphibole schists hosted in kyanite-bearing gneisses. The sapphires of Gorgona in Xanthi

have pink to purple to blue color and occur in marbles alternating with amphibolites [21]. Samples from both deposits host spinel along with pargasite in the samples of Paranesti and zircon inclusions in the samples from Gorgona. Both occurrences are found along the ultra-high to high pressure Nestos suture zone (Figure 1). At the central part of Naxos island (Kinidaros), an outcrop with pink and blue to colorless sapphires, is found in desilicified granite pegmatite (e.g., plumasite) intruding an ultrabasite, and in associated metasomatic reaction zones [21]. These sapphires are characterized by inclusions of margarite, diaspore, phlogopite, chlorite, apatite and zircon. Sapphires from Ikaria Island are hosted within extensional fissures of Mesozoic metabauxites incorporated in marbles and they include ilmenite, rutile, ulvöspinel, hematite, chloritoid and zircon.

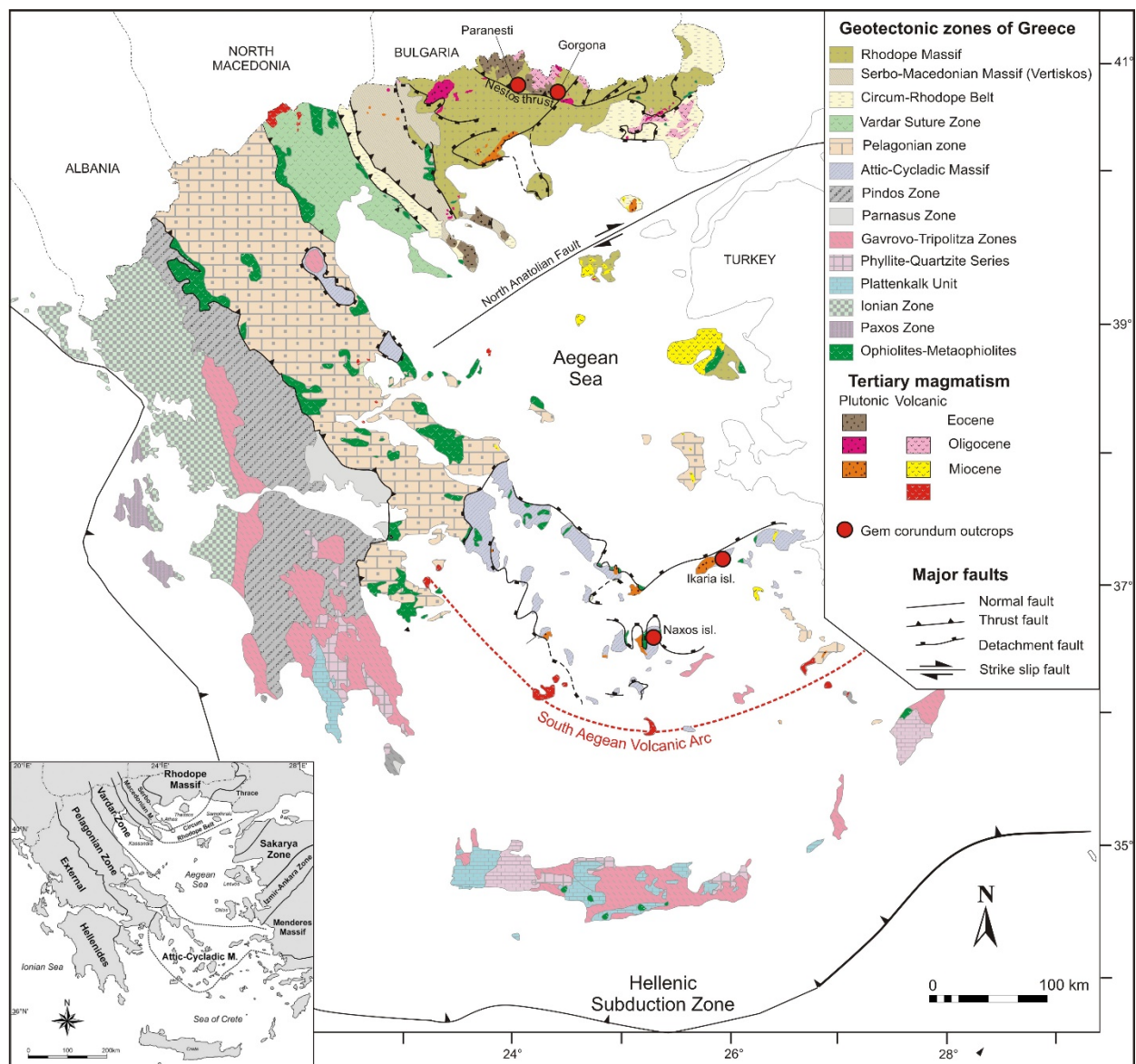


Figure 1. Simplified map of Greece showing the main geotectonic zones, the major tectonic structures within the Hellenides, and the distribution of the gem corundum (rubies and sapphires) in Paranesti, Gorgona, Ikaria island and Naxos island of Greece. The geotectonic zones of the Hellenic orogen are shown in the inset.

Based on their trace element concentrations, Greek sapphires were formed at various geological settings [21]. For instance, the Paranesti and Gorgona samples are classified as metamorphic sapphires, while those from Kinidaros (central Naxos) are of metasomatic

origin. The sapphires from Ikaria exhibit an atypical magmatic signature indicating a metasomatic origin by fluid–rock interaction.

Most gem quality samples are studied using mainly non-destructive methods for their characterization [28,29]. The purpose of the present work is to study some of the limited sapphires from Greece found in situ in primary rocks, applying non-destructive methods, commonly used by gemologists, such as FTIR, UV-Vis and EDXRF as well as optical microscopy. This study expands previous works [21] which presented detailed information on the geology, mineralogy, geochemistry, O-isotopes and fluid characteristics involved in the formation of Greek corundum.

2. Materials and Methods

Eight rare sapphires from four different primary occurrences in Greece were chosen for this study (Figure 2). Two samples are of pink color from Paranesti in Drama (DR1a slightly red, PARa; Figure 2a,b, respectively), one light pink and one light blue to blue sample from Gorgona in Xanthi (GO5a slightly purple, GORa; Figure 2c,d, respectively), one light blue to blue sample from Ikaria (IK1b) (Figure 2e) and three colorless to blue samples from Kinidaros at the central part of Naxos island (NX1a colorless to light blue, NX2a colorless to blue, NX4a colorless to blue; see Figure 2f–h). All these samples were collected by some of the authors (7 samples by PV and 1 sample by VM) and were previously studied in terms of mineralogy, mineral chemistry, fluid inclusions and oxygen isotopes [21]. The samples were cut into the appropriate size and double polished thin sections were prepared (thicknesses of the samples are stated in the caption of Figure 2). Petrographic and mineralogical observations were made using a Carl Zeiss Axioskop 40 microscope (Carl Zeiss GmbH, Oberkochen, Germany) at various magnifications.

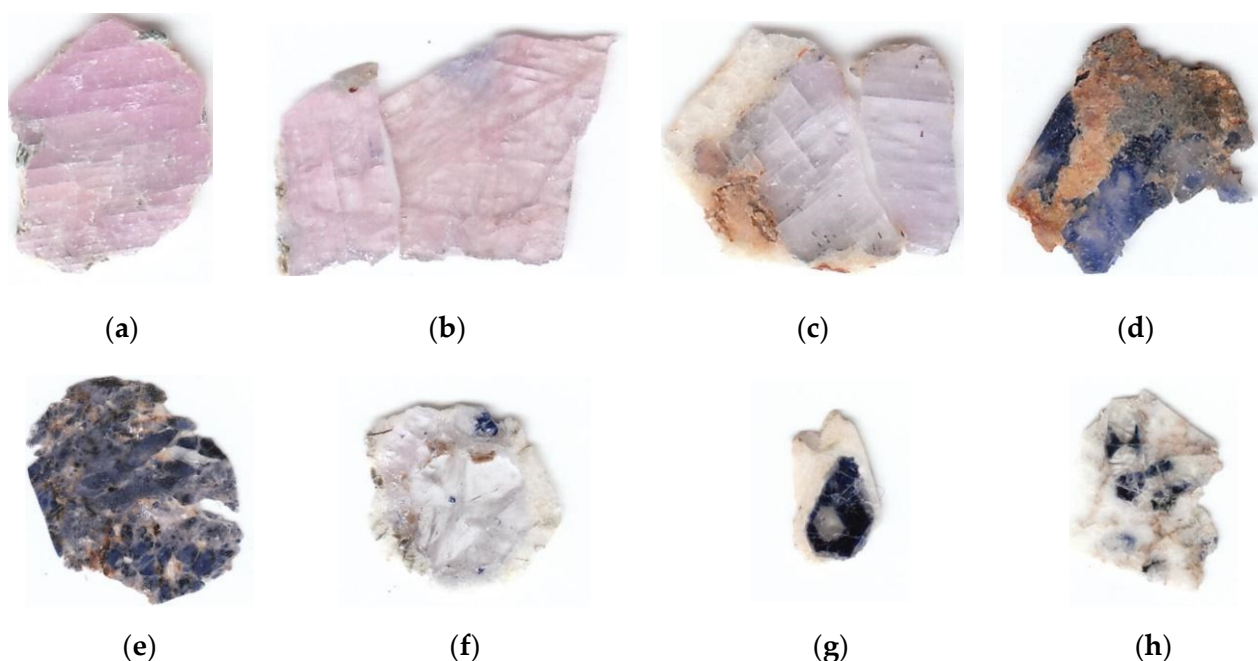


Figure 2. Photographs of the eight studied corundum samples from Greece. (a,b) Transparent to translucent pink sapphires hosted in amphibole schist from Paranesti in Drama (samples DR1a-a; slightly red, sized 8 cm × 7 cm × 0.6 cm and PARa-b, broken in two pieces, total size 12 cm × 10 cm × 0.5 cm); (c) transparent to translucent pink (slightly purple) sapphire hosted in marble from Gorgona in Xanthi (sample GO5a broken in two pieces) total size 10 cm × 7.5 cm × 0.6 cm; (d) transparent to translucent sapphire hosted in marble from Gorgona in Xanthi (sample GORa) sized 11 cm × 8 cm × 0.4 cm; (e) transparent to translucent light blue to blue sapphire hosted in meta-bauxite from Ikaria island (sample IK1b sample) sized 16 cm × 2.5 cm × 0.2 cm; (f–h) transparent to translucent colorless to blue sapphires hosted in plumasite from Kinidaros, Naxos island (samples NX1a-f, sized 9.5 cm × 8 cm × 0.5 cm, NX2a-g, sized 7.5 cm × 4 cm × 0.6 cm and NX4a-h, sized 10 cm × 4 cm × 0.5 cm).

Unpolarized FTIR spectra were acquired using a Perkin Elmer 100S spectrometer (Perkin Elmer, Waltham, MA, USA) from 400 to 8500 cm^{-1} , with a spectral resolution of 4 cm^{-1} and 100 scans (background spectra were acquired using the same parameters). Unpolarized UV-Vis spectra were conducted by a Cary 5000 (Agilent Technologies, Santa Clara, CA, USA) from 250 to 850 nm, with a data interval (DI) and spectral bandwidth (SBW) of 0.7 nm and 210 nm/min scan rate (background spectra were acquired using the same parameters). All FTIR and UV-Vis spectra presented here were acquired on colored zones. Absorption coefficient (α) is presented for all FTIR and UV-Vis spectra which is equal $\alpha = 2.303 \times A/t$; where A: absorption and t: sample thickness in cm. EDXRF analyses were carried out, on different colored zones, with an ARL Quant'X c (Thermo Fisher Scientific, Waltham, MA, USA), using a special set of parameters optimized for the analysis of corundum with various conditions of voltage (six steps from 5 to 30 kV), lifetime (200–300 s), and filter type (no filter, cellulose, aluminum, palladium). The measured trace elements for this study are Ti, V, Cr, Fe and the detection limits for these elements are of about 10 ppm.

3. Results

3.1. Microscopy

Pink colored samples DR1a and PARa from Paranești are fractured or brecciated and exhibit clear parting and polysynthetic twinning (Figure 3a). Green chlorite, demonstrating pleochroism and anomalous interference colors, fills the cracks in corundum (Figure 3b). Samples GORa and GO5a from Gorgona in Xanthi are also heavily fractured or brecciated, with clear parting and polysynthetic twinning (Figure 3c,d). They contain kyanite and allanite inclusions, up to 2 mm and 150 μm long, respectively (Figure 3e,f).

The studied sapphire outcrop from Ikaria (IK1b) occurs in granular masses of anhedral and euhedral crystals varying in size up to 3 mm (Figure 3g). Inclusions of colorless micaceous margarite and brown biotite are observed, filling the cavities among the grains of the sample (Figure 3g,h). Biotite is locally replaced by chlorite (Figure 3h). Sapphires from Naxos island (NX1a, NX2a and NX4a) form hexagonal euhedral crystals (Figure 3i,j) and are characterized by polysynthetic twinning. The crystals sometimes exhibit a zoning with a blue color core surrounded by a colorless rim, or reversely (Figure 3i,j). Interference figure taken in the colorless inner part of a blue-rimmed corundum is uniaxial with a small separation of the isogyres possibly indicating strain. Commonly, sapphires from Naxos contain inclusions of biotite (Figure 3k), zircon and chlorites exhibiting anomalous interference colors (Figure 3l). Numerous fluid inclusions are also observed in the studied samples [21].

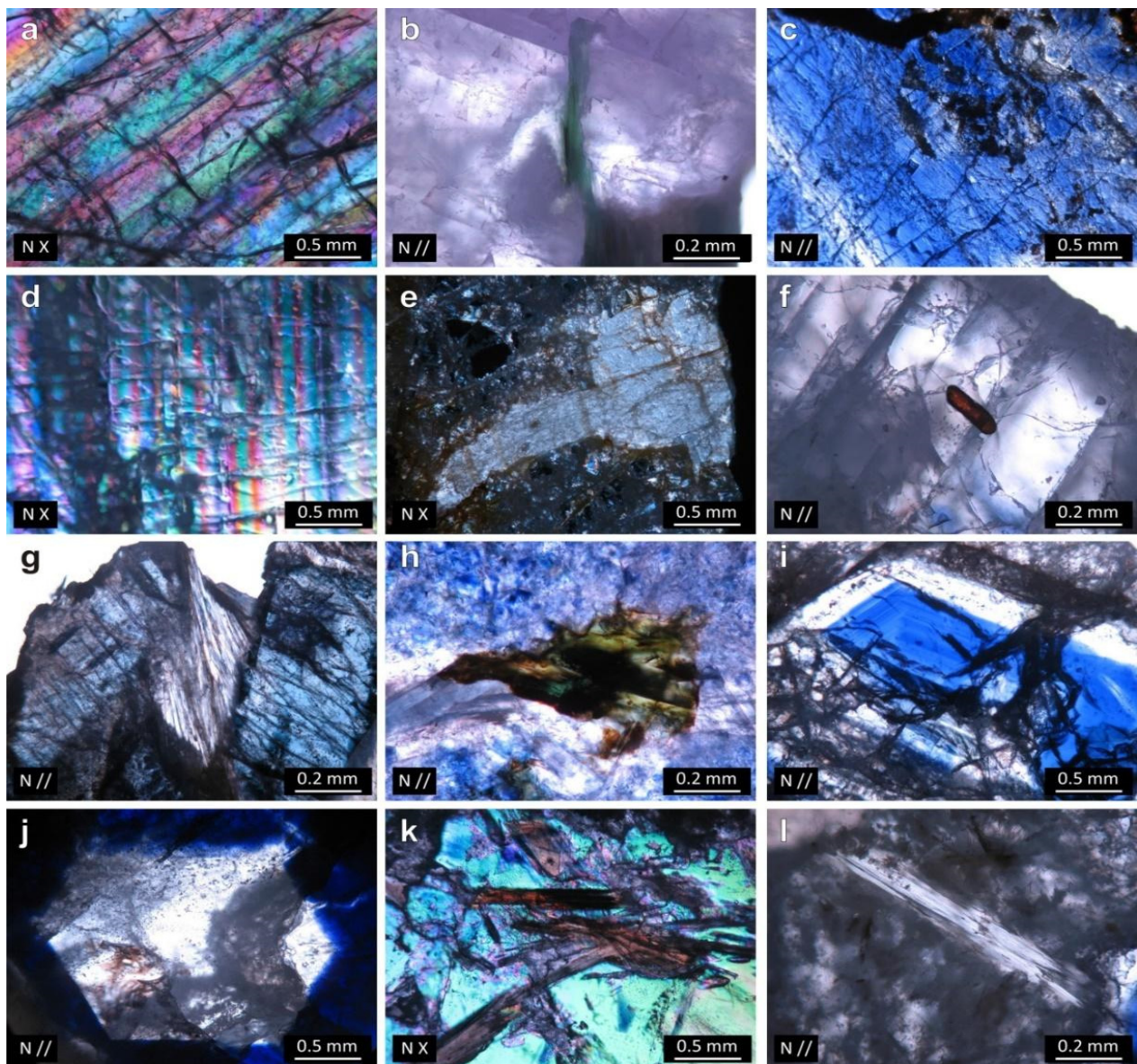


Figure 3. Microphotographs of thin sections of the studied corundum from Greece under transmitted polarized light microscope. N// = parallel nicols; NX = crossed nicols. (a) Parting and polysynthetic twinning in sample DR1a from Paranesti; (b) chlorites filling a crack in sample DR1a from Paranesti; (c) heavily fractured blue color corundum crystal, exhibiting strong pleochroism (sample GORa); (d) partings and polysynthetic twinning in pink sapphire from Gorgona (sample GO5a); (e) kyanite crystal in sapphire from Gorgona (sample GORa); (f) allanite inclusion in corundum from Gorgona (sample GO5a); (g) two euhedral blue corundum crystals with a margarite inclusion in between (sample IK1b); (h) biotite inclusion replaced by chlorite in sapphire from Ikaria (sample IK1b); (i) hexagonal euhedral corundum crystal with a blue core surrounded by a colorless rim (sample NX2a) from Naxos (Kinidaros); (j) sapphire from Naxos (Kinidaros) exhibiting a colorless core surrounded by a blue rim (sample NX2a); (k) biotite inclusions in a corundum crystal from Naxos (Kinidaros, sample NX1a); (l) chlorite with anomalous interference colors included in a sapphire crystal from Naxos (Kinidaros, sample NX4a).

3.2. FTIR Spectroscopy

The vast majority of bands are present above 1500 cm^{-1} in sapphires and are related to mineral inclusions (e.g., diaspore, boehmite, mica, chlorite, titanite, apatite) [2,30–34]. In Figures 4–6 the FTIR absorption spectra from 1500 to 4000 cm^{-1} of the studied samples are presented.

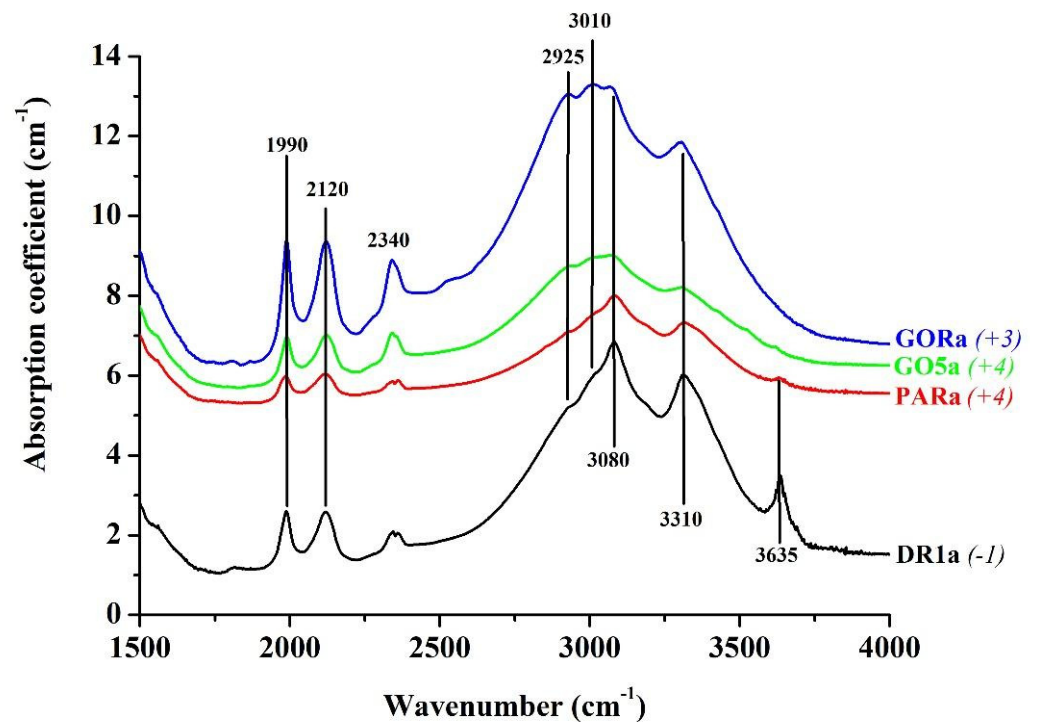


Figure 4. FTIR spectra of the samples DR1a (black trace), PARa (red trace), GO5a (green trace) and GORa (blue trace). All spectra are shifted vertically (value in parenthesis) for clarity.

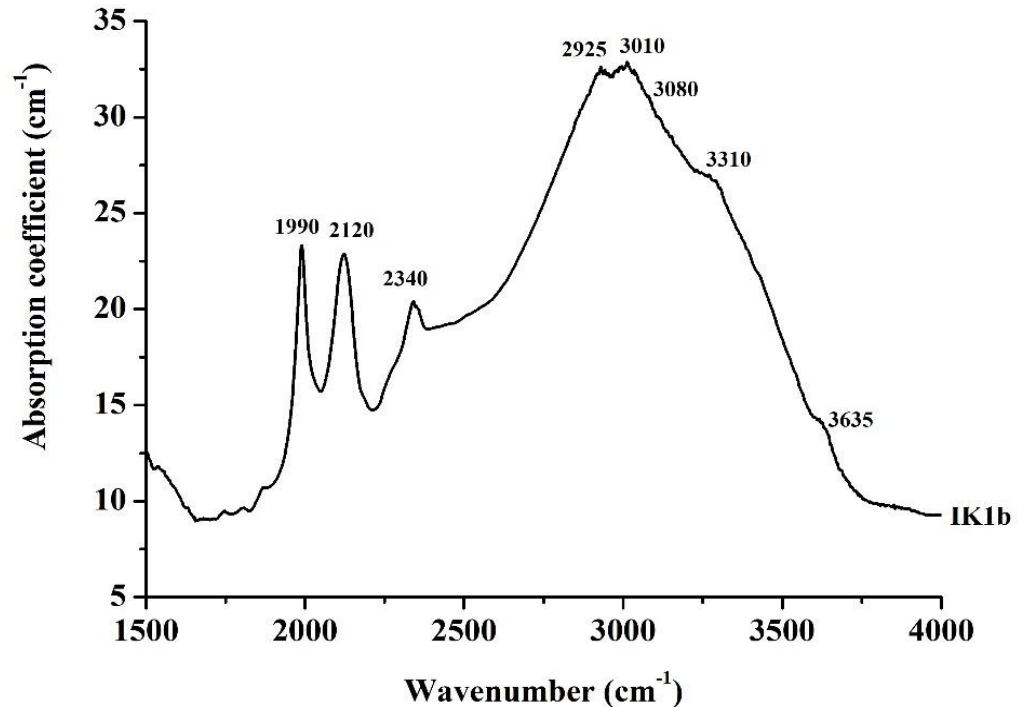


Figure 5. FTIR spectrum of the sample IK1b.

In Figure 4, the FTIR spectra of the two pink sapphires from Paranesti in Drama (DR1a and PARa) along with a pink (GO5a) and a blue (GORa) sapphire from Gorgona in Xanthi are presented. The most intense absorptions are observed above 3000 cm^{-1} . All four spectra present similar bands with different relative intensities. For the samples from Paranesti in Drama the main apparent maxima are centered at about 3080 and 3310 cm^{-1} .

These bands are due to OH vibrations of boehmite inclusions [2]. Bands at the same position also appear in the samples from Gorgona in Xanthi. Additional bands appear at around 2925 and 3010 cm^{-1} in all four spectra. They are more pronounced in the samples from Gorgona at Xanthi and are related to diaspore inclusions [2,30,34]. Two bands linked to diaspore inclusions at around 1990 and 2120 cm^{-1} are also observed in all four samples. A weak band at around 3370 cm^{-1} and a second band situated around 3145 cm^{-1} , due to OH vibrations of goethite inclusions, are also possibly present but they are hidden by the rest of the bands which are more intense bands [2]. A band at around 3635 cm^{-1} is clearly seen for DR1a and is less intense for the sample PARa. On the other hand, two bands with lower intensity are observed for the sample GO5a at around 3520 and 3620 cm^{-1} . These bands are related to OH vibrations of mica and/or chlorite inclusions in the studied samples [30,35]. A band at around 2350 cm^{-1} , which is actually a doublet, is observed for all four samples. This band could be spurious, not specimen related, associated with atmospheric CO_2 and/or due to CO_2 from the fluid inclusions [2,36]. The CO_2 related band in the studied samples is with important intensity and with relatively large full width half maximum (FWHM; bands due to atmospheric CO_2 are in general sharper with smaller FWHM compared to those due to CO_2 of inclusions). Taking also into account the presence of numerous fluid inclusions in the studied samples [21], these bands are most probably attributed to vibrations related to CO_2 from the fluid inclusions.

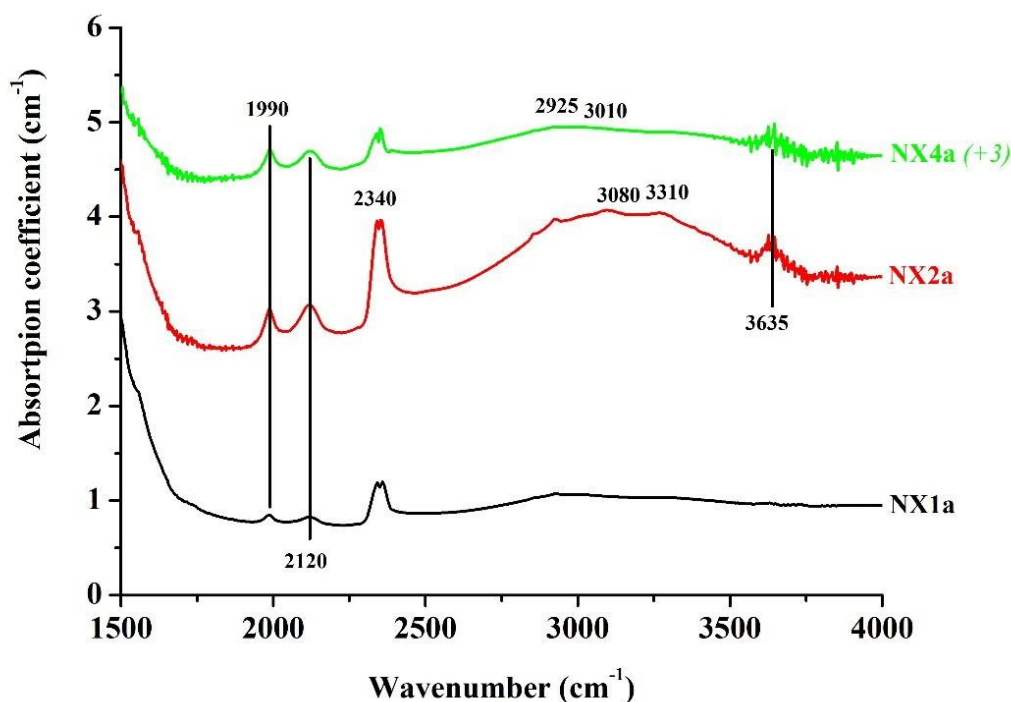


Figure 6. FTIR spectra of the samples NX1a (black trace), NX2a (red trace) and NX4a (green trace). The green spectrum is shifted vertically (value in parenthesis) for clarity.

In Figure 5, the FTIR spectrum of the sapphire from Ikaria Island (IK1b) is presented. All absorption bands are similar to those observed to Figure 4, but for this sample the diaspore related bands situated at 2925 and 3010 cm^{-1} along with those at 1990 and 2120 cm^{-1} , are the most intense. Bands due to CO_2 -rich fluid inclusions, boehmite, mica and/or chlorites are also observed. All bands for IK1b present a relatively important absorption coefficient, which indicates that the above-mentioned inclusions are possibly more pronounced in this sample. In Figure 6 the FTIR spectra of the three sapphires (from very light blue to blue color) from Naxos island are shown. These samples exhibit the same bands described above but with the lower absorption coefficient. Only the sample NX2a exhibits CO_2 related bands with relatively important intensity.

From 3500 to 4000 cm^{-1} , apart from the 3635 cm^{-1} band, the signal to noise ratio is low due to spurious H_2O instrument related bands. Above 4000 cm^{-1} the sample DR1a presents absorptions at around 4540 cm^{-1} , possibly due to 3635 cm^{-1} combination/overtone bands.

3.3. UV-Vis Spectroscopy

Figures 7–10 show the UV-Vis absorption spectra from 250 to 850 nm of the studied samples. At the pink sapphires from Paranesti (PARa and DR1a, with the latter being slightly red) two large absorptions at 405 and 560 nm, as well as a weak sharp band at around 694 nm (a doublet called “R1 and R2 lines”), are observed (Figure 7). The absorptions are linked to Cr^{+3} which usually gives a pink to red color to sapphire [1–3,5,37]. Additional weak sharp bands appear at 377 and 450 nm, due to Fe^{+3} - Fe^{+3} pairs and at 388 nm, due to single Fe^{+3} ions [1–3,38–42]. In the ultraviolet (UV) region of the electromagnetic spectrum, a cut off (absorption edge as known as total/full absorption) at around 300 nm (295 nm for DR1a and at 305 nm for PARa) along with an intense shoulder, of debatable origin, at around 335 nm are observed [2].

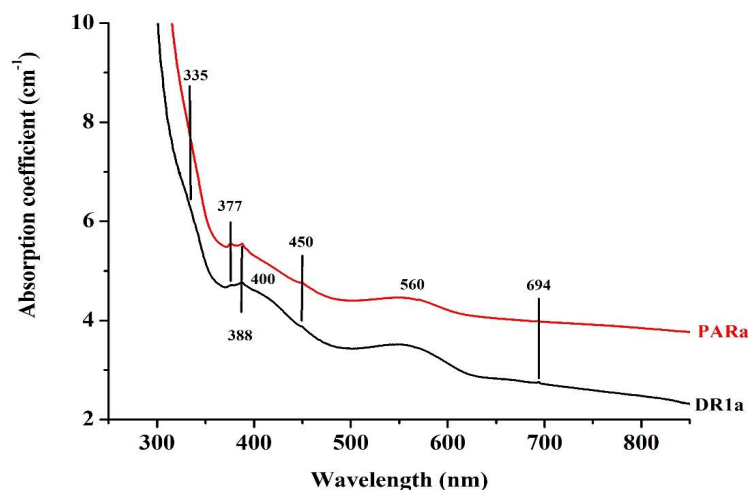


Figure 7. UV-Vis spectra of the samples DR1a (black trace) and PARa (red trace), both of pink color with DR1a being slightly red, from Paranesti (Drama).

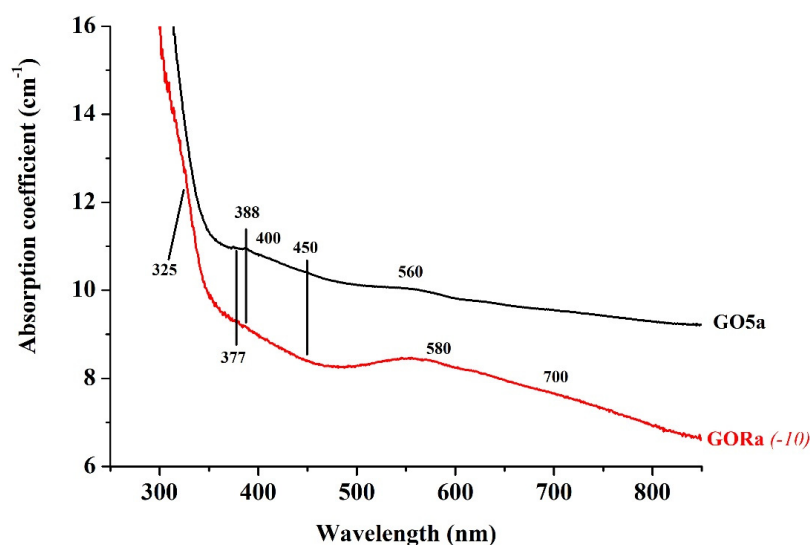


Figure 8. UV-Vis spectra of the pink (slightly purple) sample GO5a (black trace) and the blue sample GORa (red trace) from Gorgona (Xanthi). Red spectrum is shifted vertically (value in parenthesis) for clarity.

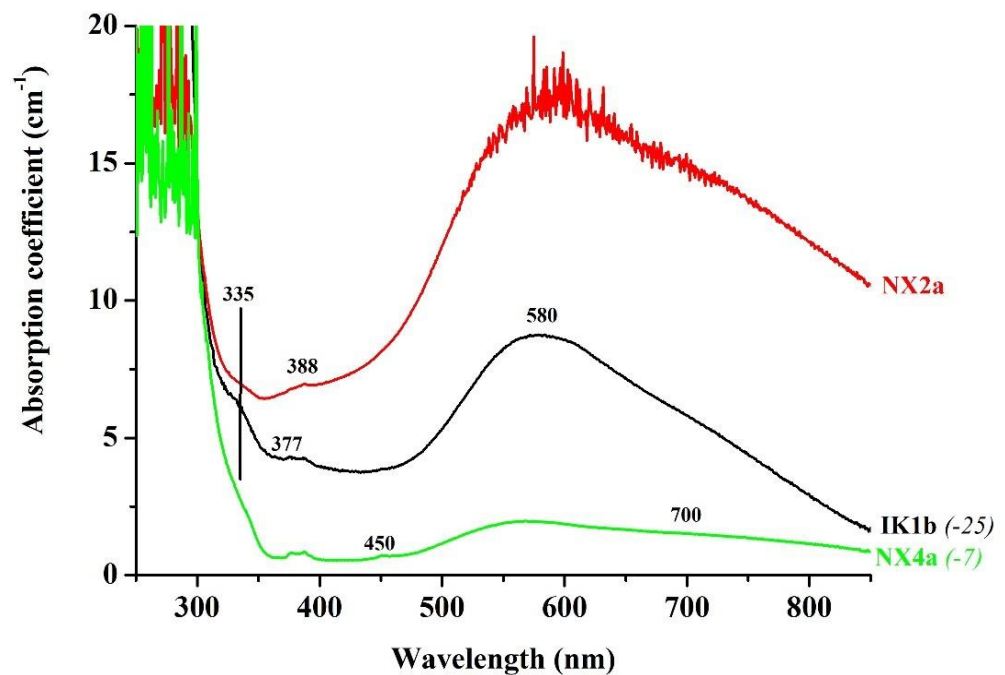


Figure 9. UV-Vis spectra of sapphires from Ikaria and (Kinidaros) Naxos islands; IK1b (black trace), NX2a (red trace) and NX4a (green trace). Black and green spectra are shifted vertically (value in parenthesis) for clarity.

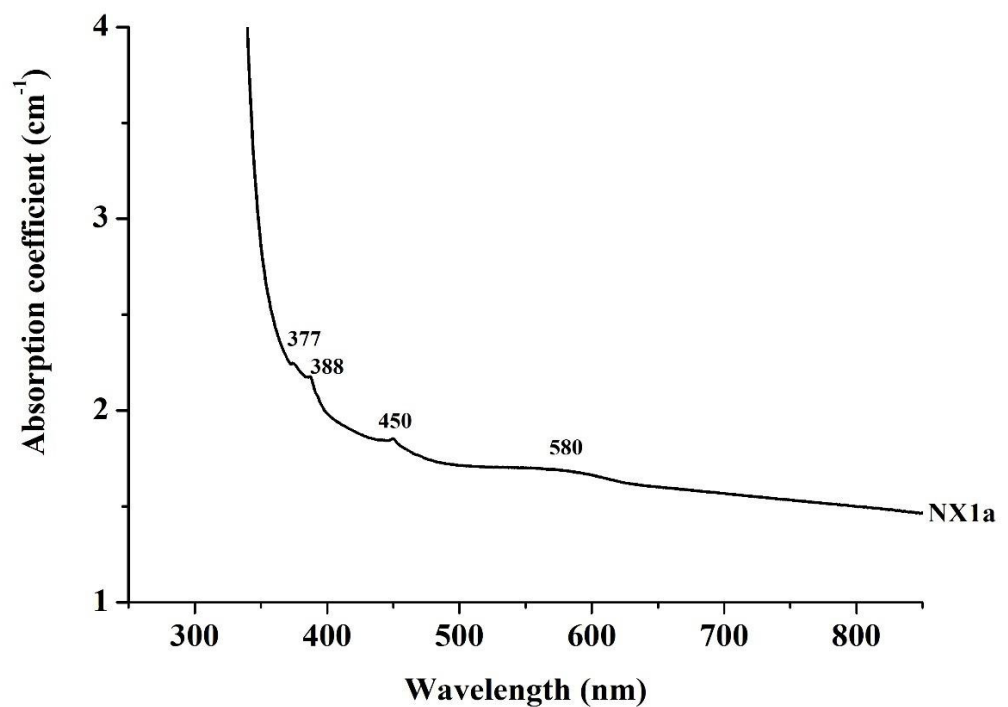


Figure 10. UV-Vis spectra from 250 to 850 nm of the light colored sapphire NX1a from (Kinidaros) Naxos Island.

Figure 8 exhibits the absorption spectra of the light pink, slightly purple, sapphire GO5a and the blue sapphire GORa from Gorgona. Sample GO5a shows the same absorption bands in the visible range as the samples presented in Figure 7, with the chromium related bands situated at 400 and 560 nm and the iron related narrow bands situated at 377, 388 and 450 nm having lower intensity. Chromium related bands do not appear in the spectrum

of the blue colored GORa sample; only the Fe^{+3} related bands at 377, 388 and 450 nm. Additionally, a broad absorption from 500 to 750 nm is observed with apparent maxima at around 580 nm and another at around 700 nm. These bands are responsible for the blue color and are related to intervalence charge-transfer by $\text{Fe}^{2+}\text{-Ti}^{4+}$ [2,41–45]. The cut off for the sample GO5a is at around 310 nm and for the sample GORa at around 295 nm. The latter is also presenting a shoulder at around 325 nm.

In Figure 9, UV-Vis absorption spectra of the blue colored samples IK1b, NX2a and NX4a are displayed. Fe^{+3} related narrow absorptions at 377, 388 and 450 nm are detected for all the samples as well as the large absorptions due to $\text{Fe}^{2+}\text{-Ti}^{4+}$ pairs situated at 580 and 700 nm. In sample NX4a Fe^{+3} related absorptions are clearly apparent with the bands due to $\text{Fe}^{2+}\text{-Ti}^{4+}$ pairs having lower intensity compared to those observed for IK1b and NX2a. On the other hand, the NX2a sample presents the more intense bands due to $\text{Fe}^{2+}\text{-Ti}^{4+}$ pairs which causes a relatively “noisy” signal due to spectrometer’s detector saturation. The Fe^{+3} related bands are barely seen in this sample. All three samples in this figure exhibit the cut off at around 300 nm and a shoulder of various intensities at around 335 nm. In Figure 10 the absorption spectrum of the light blue colored sapphire NX1a, demonstrates bands at 377, 388, 450 and 580 nm, similar to the samples of Figure 9. No band at 700 nm is observed, possibly because of the sample’s light color as well as its crystallographic orientation (absorption bands due to $\text{Fe}^{2+}\text{-Ti}^{4+}$ pairs present strongly polarized phenomena [3]). NX1a presents a cut off situated at 330 nm but no shoulder is apparent in the UV region of the electromagnetic spectrum.

3.4. EDXRF

Table 1 presents the concentrations of titanium, chromium, iron and gallium oxides measured in the studied corundum samples. Vanadium is below EDXRF’s detection limit in all samples. Chromium is present only in the studied samples from Paranesti (Drama), in sample GO5a from Gorgona (Xanthi) and in sample IK1b from Ikaria Island.

Pink sapphires from Paranesti (Drama) have a relatively high Cr_2O_3 content ranging between 598 and 1213 ppm (or $\mu\text{g/g}$; 1000 ppm = 0.1 wt.%). The high chromium concentration in these samples is associated with their pink to red color. The sample DR1a demonstrates relatively low TiO_2 (52 and 131 ppm) whereas sample PARa contains slightly higher concentrations from 206 to 709 ppm. The two samples from Paranesti present relatively high Fe_2O_3 with values ranging from 0.3049 to 0.5461 wt. % and relatively low Ga_2O_3 content from 28 to 38 ppm.

The range of TiO_2 compositions of sapphires from Gorgona (Xanthi) is 144–662 ppm, with one outlier of 6030 ppm, probably due to inclusions (e.g., rutile). The Fe_2O_3 content ranges between 0.0128 and 1.4414 wt. %; these high values are possibly associated with iron rich inclusions (e.g., allanite). The Cr_2O_3 content of two light pink (slightly purple) colored points of sample GO5a is 255 and 311 ppm. On the other hand, Cr_2O_3 is below the detection limit in blue sample GORa and some points of GO5a. Ga_2O_3 is relatively low in both samples and varies from 37 to 43 ppm in GORa and from 51 to 130 ppm in GO5a.

The sapphire IK1a from Ikaria island shows a TiO_2 concentration from 0.1696 to 0.2138 wt. %, relatively high Fe_2O_3 content (0.4464 to 0.6561 wt. %) and Ga_2O_3 from 93 to 112 ppm. The Cr_2O_3 content ranges between 242 and 453 ppm, having no effect on the color of the studied sample; instead, the sample’s blue coloration results from its relatively high iron and titanium content.

The studied samples from (Kinidaros) Naxos Island also demonstrate relatively high iron concentrations (up to 0.7216 wt. % Fe_2O_3). The TiO_2 content reaches up to 0.6065 wt. %. The highest values are observed for the colorless to light blue colored sample NX1a ranging from 0.2263 to 0.6065 wt. %; possibly because of titanium rich inclusions (e.g., rutile). Samples NX2a and NX4a present TiO_2 up to 0.1030 wt.%. They also have relatively higher Fe_2O_3 values than sample NX1a, possibly linked to the more intense blue color. The Ga_2O_3 content of the studied samples from Naxos Island lies between 73 and 117 ppm.

Table 1. EDXRF analyses of selected oxides of trace elements in corundum from Paranesti, Gorgona, Ikaria and Naxos (Kinidaros) in wt. %. Analyses were acquired on different colored points; Bdl: below detection limit.

Region	Sample	TiO ₂	Cr ₂ O ₃	Fe ₂ O ₃	Ga ₂ O ₃
Paranesti	DR1a	0.0131	0.1107	0.3058	0.0031
		0.0052	0.1173	0.3049	0.0034
	PARa	0.0709	0.0639	0.4192	0.0028
		0.0414	0.0598	0.4509	0.0029
		0.0686	0.0685	0.3883	0.0036
Gorgona	GO5a	0.0206	0.1213	0.5461	0.0038
		0.0522	Bdl	0.1503	0.0103
		0.0421	Bdl	0.1785	0.0130
		0.6030	0.0311	0.1449	0.0085
		0.0144	0.0255	0.1404	0.0099
	GORa	0.0224	Bdl	0.0340	0.0051
		0.0261	Bdl	0.0128	0.0085
		0.0449	Bdl	0.1210	0.0037
		0.0662	Bdl	0.1015	0.0042
		0.1099	Bdl	0.9721	0.0043
Ikaria	IK1b	0.1020	Bdl	1.4414	0.0040
		0.1696	0.0453	0.4464	0.0093
		0.1787	0.0357	0.4953	0.0112
Naxos	NX1a	0.2138	0.0242	0.6561	0.0106
		0.3713	Bdl	0.3288	0.0077
		0.6065	Bdl	0.3277	0.0094
		0.4614	Bdl	0.3230	0.0084
		0.3817	Bdl	0.3470	0.0092
		0.3816	Bdl	0.3356	0.0080
	NX2a	0.2263	Bdl	0.3943	0.0074
		0.0202	Bdl	0.5567	0.0108
		0.1030	Bdl	0.6028	0.0077
		0.0471	Bdl	0.6365	0.0073
		Bdl	Bdl	0.4996	0.089
		Bdl	Bdl	0.5094	0.075
NX4a	0.0580	Bdl	0.5980	0.0078	
	0.0974	Bdl	0.7216	0.0117	

4. Discussion

The present work shows that under the polarizing optical microscope all the studied corundum samples from Greece have similar features (Table 2), in agreement to previous studies [21]. Color zoning is prominent in all samples, and especially in the sapphires from central Naxos (Kinidaros), with a blue core surrounded by a colorless rim or a colorless core rimmed by a blue-colored outer zone. Apart from the Ikaria sapphire (IK1b) and one from Naxos (NX4a), all the other samples present polysynthetic twinning under crossed nicols. Parting is observed in all samples, except sample NX1 from Naxos. For a crystal to be a gem, there must have been no dramatic syn- or post-growth events before either the crystal reaches the surface or is mined underground [46]. All studied corundum samples are highly fractured and brecciated, indicating high brittle deformational conditions that occurred after their crystallization. This limits the gem quality of the studied samples. It looks as though only small crystals from these localities might be of gem quality and that bigger crystals of better appearance might be produced after treatment (e.g., heat treatment in flux).

The studied corundum samples from Greece also contain various mineral inclusions identified under polarizing optical microscope (Table 3). In the pink sapphires from Paranesti only traces of chlorite inclusions are observed (sample DR1a). Previous studies have shown that they also include spinel and pargasite. Allanite inclusions were seldomly recognized in the Gorgona sapphire (sample GO5a), as well as traces of an opaque mineral

(possibly spinel) [21]. The presence of kyanite in Gorgona (sample GORa) complies with the regional geology and the presence of corundum-bearing marbles alternating with eclogitic amphibolites and kyanite-bearing eclogites [47]. According to earlier studies in Gorgona, pink to purple to blue sapphires can also include spinel and zircon [21]. The studied Ikaria sapphire is characterized by the presence of biotite, white mica (possibly margarite), chlorite and unidentified opaque minerals. These microscopic observations are in agreement with previous observations which identified inclusions of margarite, chloritoid, ilmenite, hematite, ulvöspinel, rutile and zircon [21]. The Kinidaros (central part of Naxos island) studied sapphires contain various minerals including biotite, chlorite, zircon, needle-like rutile and opaque phases. Nearly similar inclusions (margarite, zircon, apatite, diaspore, phlogopite, chlorite) in the corundum of the central part of Naxos Island (Kinidaros) were also previously reported [21].

Table 2. Characteristic features of the Greek corundum studied under transmitted light microscope.

Region	Sample	Polysynthetic Twinning	Parting	Color Zoning	Fractures
Paranesti	DR1a	+	+	+	+
	PARa	+	+	+	+
Gorgona	GO5a	+	+	+	+
	GORa	+	+	+	+
Ikaria	IK1b	-	+	+	+
	NX1a	+	-	+	+
Naxos	NX2a	+	+	+	+
	NX4a	-	+	+	+

Table 3. Mineral inclusions of the Greek corundum studied under transmitted light microscope.

Region	Sample	Biotite	White Mica	Chlorite	Kyanite	Zircon	Allanite	Rutile	Opaque Minerals
Paranesti	DR1a	-	-	+	-	-	-	-	-
	PARa	-	-	-	-	-	-	-	-
Gorgona	GO5a	-	-	-	-	-	+	-	+
	GORa	-	-	-	+	-	-	-	+
Ikaria	IK1b	+	+	+	-	-	-	-	+
Naxos	NX1a	+	-	-	-	+	-	-	+
	NX2a	+	-	-	-	-	-	+	-
	NX4a	+	-	+	-	-	-	-	-

Using FTIR spectroscopy, pronounced vibrations due to hydroxyl in boehmite, diaspore, goethite, mica and/or chlorite inclusions are observed above 3000 cm^{-1} , along with bands at around 2350 cm^{-1} , because of CO_2 from fluid inclusions, for all the studied samples. The relative intensities of these absorptions differ from sample to sample. Boehmite bands are prominent on the samples from Paranesti. On the other hand, the Ikaria sample presents intense diaspore-related absorption bands. The samples from Gorgona and Naxos (Kinidaros) present boehmite and diaspore infrared absorptions of similar relative intensities. However, the diaspore and boehmite inclusions were not observed under microscope in this study. Diaspore has been previously mentioned in the paragenesis for some of the corundum occurrences from Naxos [21]. Boehmite inclusions are frequently situated along corundum twinning planes [48]. Both, boehmite and diaspore, inclusions are most likely epigenetic (i.e., grown after corundum formation) in the studied samples and have been previously observed in the FTIR spectra of corundum from various localities elsewhere such as in rubies from Mong Hsu (Burma/Myanmar), in sapphires from Baw Mar (Burma/Myanmar) and sapphires from Ilmen Mountains (South Urals, Russia) [6,9,28,34,48,49]. Moreover, the samples from Paranesti and Naxos present the most intense mica and/or chlorite FTIR bands. The samples from Naxos demonstrate also the most important CO_2 bands. A detailed fluid inclusions study in the Greek corundum

showed that they are dominated by pure CO₂ with very small quantities of CH₄ and/or N₂ and are water-free [21].

The studied corundum samples from Greece contain various bands in the ultraviolet and visible range of the electromagnetic spectrum (Table 4). The pink colored samples from Paranesti (DR1a, PARa) present a weak and hardly visible shoulder at around 335 nm while those from Gorgona (GO5a) demonstrate no shoulder in the UV region. A total absorption (“cut off”) in GO5a is visible at around 310 nm, while in DR1a and PARa at around 295 and 305 nm, respectively. Samples from Paranesti (DR1a, PARa) present Cr³⁺ related absorptions of medium intensity centered in the violet (at 405 nm) and yellow-green (at 560 nm) part, along with a weak sharp doublet in the red part, of the electromagnetic spectrum which causes their pink color. These bands are slightly more intense for sample DR1a which is in agreement with the slight red color. Weak bands related to Fe³⁺ in the violet and blue part of the electromagnetic spectrum are also observed for both samples at 377, 388 and 450 nm. The sample GO5a presents bands related to Cr³⁺ and Fe³⁺ of weak intensities, possibly along with very weak bands (not visible in the acquired spectrum) centered in the yellow-orange (at 580 nm) and red (at 700 nm) due to intervalence charge-transfer by Fe²⁺-Ti⁴⁺, which causes the pink hue of the sample.

Table 4. Features and absorption peaks in nm obtained with UV-Vis spectroscopy from all studied samples.

Region	Sample	“Cut off” UV Region	“Shoulder” UV Region	377/450 Fe ³⁺ -Fe ³⁺	388 Fe ³⁺	580/700 Fe ²⁺ -Ti ⁴⁺	405/560 Cr ³⁺
Paranesti	DR1a	295	335	Weak	Weak	-	Medium
	PARa	305	335	Weak	Weak	-	Medium
Gorgona	GO5a	310	-	Weak	Weak	Weak?	Weak
	GORa	295	325	Weak	Weak	Medium	-
Ikaria	IK1b	300	335	Weak	Weak	Strong	-
Naxos	NX1a	330	-	Weak	Weak	Weak	-
	NX2a	300	335	Weak	Weak	Strong	-
	NX4a	300	335	Weak	Weak	Medium	-

UV-Vis spectra of blue sapphires can give valuable information regarding their host geological environment [2,13,28,29,50,51]. Basalt-related sapphires are known to present a broad band at around 880 nm of higher intensity compared to those observed at around 580 nm due to Fe²⁺-Ti⁴⁺. The cause of the band at 880 nm is still under discussion with intervalence charge-transfer by Fe²⁺-Fe³⁺ as a possibility [52]. None of the studied sapphires present this band, excluding a possible basaltic origin. Four studied samples (GORa, IK1b, NX2a and NX4a) show a shoulder at around 335 nm (the GORa at 325 nm) of various intensities. Despite the fact that this shoulder is of debatable origin, its presence denotes the metamorphic or metasomatic origin of the samples [50,51]. All studied sapphires present a complete absorption (“cut off”) situated from 295 to 300 nm; only the light blue colored sample NX1a demonstrates a “cut off” at around 330 nm without the presence of shoulder. In earlier studies [21] it has been concluded that the Paranesti, Gorgona and central Naxos corundum deposits are classified as metamorphic and metasomatic, respectively, while those from Ikaria display atypical magmatic signature indicating a hydrothermal origin.

The chemical analyses of blue colored samples show important contents of titanium and iron which are linked to their color. However, the high titanium and high iron concentrations of some of the studied samples are most probably related to certain mineral inclusions. These inclusions can affect chemical compositions and lead to wrong interpretations; thus, analyses of inclusion-free areas are needed to better understand sapphires’ geochemical character [8,9]. The Cr₂O₃ content is associated with the pink color of the corundum from Paranesti and Gorgona. In most blue sapphires, chromium is below the detection limit of EDXRF, apart from sample IK1b. The color of this sample is affected by iron and titanium, which are in higher values than chromium. No absorption in the visible range is observed due to chromium, but absorption due to iron and titanium are

detected; therefore, chromium does not contribute to the color (see again Figure 9). The samples from Paranesti and the blue sample from Gorgona (GORa) show also relatively lower values of Ga_2O_3 than the pink sample from Gorgona (GO5a) and the blue samples from Ikaria and central Naxos. These variations suggest a possible polygenetic (distinct) geologic origin of the pink and blue sapphires from Gorgona [19].

5. Conclusions and Perspectives

The four studied corundum deposits from Greece in Paranesti (Drama), Gorgona (Xanthi), Ikaria and Kinidaros (central Naxos) share similar features under the polarizing microscope; e.g., parting, polysynthetic twinning, color zoning and fracturing. Most of these microscopic characteristics are linked to post-crystallization deformation. This deformation limits their gem quality. FTIR spectroscopy reveals the presence of boehmite, diaspore, goethite, mica and/or chlorite inclusions along with CO_2 in fluid inclusions, for all the studied samples. The diaspore and boehmite inclusions were not observed under microscope and are most likely epigenetic. UV-Vis spectra on the studied samples further confirm that the pink color of samples from Paranesti and Gorgona is due to Cr^{3+} and the blue color of samples from Gorgona, Ikaria island and Kinidaros is due to Fe^{2+} - Ti^{4+} intervalence charge transfer. EDXRF analyses in some of the studied samples show relatively high titanium and iron concentrations related with various mineral inclusions. Gallium of the studied samples slightly differs from region to region. Moreover, blue sapphire from Gorgona is characterized by lower gallium content than the pink sapphire from the same region; this is possibly due to a polygenetic origin of the different colored sapphires from Gorgona (Xanthi).

A more detailed study, including precise geochemical analysis of more corundum samples from Greece, along with their associated minerals, as well as, detailed mapping of the areas is needed in order to better understand their exact geological formation and distribution. Further research is also needed to check the possible distinct geological origin of pink and blue colored samples from the same area (e.g., Gorgona-Xanthi). Finally, different treatments (e.g., heat treatment in flux) should be tried on Greek sapphires to check if these samples can be transformed into samples useful for the local and/or global jewelry industry.

Author Contributions: Conceptualization, P.V. and S.K.; methodology, V.K. and S.K.; investigation, V.K., P.V., S.K., V.M., T.S., L.P., C.M.; resources, P.V.; data curation, V.K., S.K. and T.S.; writing—original draft preparation, V.K., P.V., S.K., V.M., T.S., L.P., C.M.; writing—review and editing, V.K., P.V., S.K., V.M., T.S., L.P., C.M.; visualization, V.K., P.V. and S.K. All authors have read and agreed to the published version of the manuscript.

Funding: This research received no external funding.

Data Availability Statement: The data presented in this study are available on request from the corresponding author. The data are not publicly available due to privacy.

Acknowledgments: The authors acknowledge the reviewers and the editors for their constructive comments.

Conflicts of Interest: The authors declare no conflict of interest.

References

1. Fritsch, E.; Rossman, G.R. An update on color in gems. Part I. Introduction and colors caused by dispersed metal ions. *Gems Gemol.* **1987**, *23*, 126–139. [[CrossRef](#)]
2. Emmett, J.L.; Dubinsky, E.V.; Hughes, R.W.; Scarratt, K. Color, Spectra & Luminescence. In *Ruby & Sapphire: A Gemmologist's Guide*; Hughes, R., Ed.; RWH Publishing: Bangkok, Thailand, 2017; pp. 90–148.
3. Dubinsky, E.V.; Stone-Sundberg, J.; Emmett, J.L. A quantitative description of the causes of color in corundum. *Gems Gemol.* **2020**, *56*, 2–28. [[CrossRef](#)]
4. Simonet, C.; Fritsch, E.; Lasnier, B. A classification of gem corundum deposits aimed towards gem exploration. *Ore Geol. Rev.* **2008**, *34*, 127–133. [[CrossRef](#)]

5. Schwarz, D.; Pardieu, V.; Saul, J.M.; Schmetzer, K.; Laurs, B.M.; Giuliani, G.; Klemm, L.; Malsy, A.-K.; Erel, E.; Hauzenberger, C.; et al. Rubies and sapphires from Winza, central Tanzania. *Gems Gemol.* **2008**, *44*, 322–347. [[CrossRef](#)]
6. Kan-Nyunt, H.P.; Karampelas, S.; Link, K.; Thu, K.; Kiefert, L.; Hardy, P. Blue sapphires from the Baw Mar mine in Mogok. *Gems Gemol.* **2013**, *49*, 223–232. [[CrossRef](#)]
7. Giuliani, G.; Ohnenstetter, D.; Fallick, A.E.; Groat, L.; Fagan, A.J. The geology and genesis of gem corundum deposits. In *Geology of Gem Deposits*, 2nd ed.; Mineralogical Association of Canada Short Course Series; Groat, L.A., Ed.; Mineralogical Association of Canada: Tucson, AZ, USA, 2014; Volume 44, pp. 113–134. ISBN 9780921294375.
8. Palke, A.C.; Breeding, C.M. The origin of needle-like rutile inclusions in natural gem corundum: A combined EMPA, LA-ICP-MS, and nanoSIMS investigation. *Am. Mineral.* **2017**, *102*, 1451–1461. [[CrossRef](#)]
9. Sorokina, E.S.; Karampelas, S.; Nishanbaev, T.R.; Nikandrov, S.N.; Semiannikov, B.S. Sapphire megacrysts in syenite pegmatites from the Ilmen Mountains, South Urals, Russia: New mineralogical data. *Can. Mineral.* **2017**, *55*, 823–843. [[CrossRef](#)]
10. Sutherland, F. Sapphire, a not so simple gemstone. *Am. Mineral.* **2017**, *102*, 1373–1374. [[CrossRef](#)]
11. Elmaleh, E.; Schmidt, S.T.; Karampelas, S.; Link, K.; Kiefert, L.; Süßenberger, A.; Paul, A. U-Pb Ages of Zircon Inclusions in Sapphires from Ratnapura and Balangoda (Sri Lanka) and Implications for Geographic Origin. *Gems Gemol.* **2019**, *55*, 18–28. [[CrossRef](#)]
12. Giuliani, G.; Groat, L. Geology of corundum and emeralds gem deposits: A review. *Gems Gemol.* **2019**, *55*, 464–489. [[CrossRef](#)]
13. Palke, A.C.; Saeseaw, S.; Renfro, N.D.; Sun, Z.; McClure, S.F. Geographic origin determination of blue sapphire. *Gems Gemol.* **2019**, *55*, 536–579. [[CrossRef](#)]
14. Palke, A.C.; Saeseaw, S.; Renfro, N.D.; Sun, Z.; McClure, S.F. Geographic origin determination of ruby. *Gems Gemol.* **2019**, *55*, 580–612. [[CrossRef](#)]
15. Sorokina, E.S.; Rassomakhin, M.A.; Nikandrov, S.N.; Karampelas, S.; Kononkova, N.N.; Nikolaev, A.G.; Anosova, M.O.; Somsikova, A.V.; Kostitsyn, Y.A.; Kotlyarov, V.A. Origin of blue sapphire in newly discovered spinel–chlorite–muscovite rocks within meta-ultramafites of Ilmen mountains, South Urals of Russia: Evidence from mineralogy, geochemistry, Rb–Sr and Sm–Nd isotopic data. *Minerals* **2019**, *9*, 36. [[CrossRef](#)]
16. Filina, M.I.; Sorokina, E.S.; Botcharnikov, R.; Karampelas, S.; Rassomakhin, M.A.; Kononkova, N.N.; Nikolaev, A.G.; Berndt, J.; Hofmeister, W. Corundum anorthosites–kyshtymites from the South Urals, Russia: A combined mineralogical, geochemical, and U–Pb zircon geochronological study. *Minerals* **2019**, *9*, 234. [[CrossRef](#)]
17. Sutherland, F.L.; Khin, Z.; Meffre, F.; Thompson, J.; Goemann, K.; Kyaw, T.; Than, T.N.; Mhod, Z.M.; Harris, S.I. Diversity in ruby chemistry and its inclusions: Intra and inter-continental comparisons from Myanmar and Eastern Australia. *Minerals* **2019**, *9*, 28. [[CrossRef](#)]
18. Giuliani, G.; Groat, L.A.; Fallick, A.E.; Pignatelli, I.; Pardieu, V. Ruby Deposits: A Review and Geological Classification. *Minerals* **2020**, *10*, 597. [[CrossRef](#)]
19. Palke, A.C. Coexisting rubies and blue sapphires from major world deposits: A brief review of their mineralogical properties. *Minerals* **2020**, *10*, 472. [[CrossRef](#)]
20. Melfos, V.; Voudouris, P. Cenozoic metallogeny of Greece and potential for precious, critical and rare metals exploration. *Ore Geol. Rev.* **2017**, *89*, 1030–1057. [[CrossRef](#)]
21. Voudouris, P.; Mavrogatos, C.; Graham, I.; Giuliani, G.; Melfos, V.; Karampelas, S.; Karantoni, V.; Wang, K.; Tarantola, A.; Zaw, K.; et al. Gem Corundum Deposits of Greece: Geology, Mineralogy and Genesis. *Minerals* **2019**, *9*, 41. [[CrossRef](#)]
22. Voudouris, P. The minerals of Eastern Macedonia and Western Thrace: Geological framework and environment of formation. *Bull. Soc. Greece* **2005**, *37*, 62–77.
23. Voudouris, P.; Melfos, V.; Katerinopoulos, A. Precious Stones in Greece: Mineralogy and Geological Environment of Formation. Understanding the Genesis of Ore Deposits to Meet the Demand of the 21st Century. In Proceedings of the 12th Quadrennial IAGOD Symposium, Moscow, Russia, 21–24 August 2006. 6p.
24. Voudouris, P.; Graham, I.; Melfos, V.; Zaw, K.; Lin, S.; Giuliani, G.; Fallick, A.; Ionescu, M. Gem corundum deposits of Greece: Diversity, Chemistry and Origins. In Proceedings of the 13th Quadrennial IAGOD Symposium, Adelaide, Australia, 6–9 April 2010; Volume 69, pp. 429–430.
25. Graham, I.; Voudouris, P.; Melfos, V.; Zaw, K.; Meffre, S.; Sutherland, F.; Giuliani, G.; Fallick, A. Gem corundum deposits of Greece: A spectrum of compositions and origins. In Proceedings of the 34th IGC Conference, Brisbane, Australia, 5–10 August 2012.
26. Wang, K.K.; Graham, I.T.; Lay, A.; Harris, S.J.; Cohen, D.R.; Voudouris, P.; Belousova, E.; Giuliani, G.; Fallick, A.E.; Greig, A. The origin of a new pargasite–schist hosted ruby deposit from Paranesti, Northern Greece. *Can. Mineral.* **2017**, *55*, 535–560. [[CrossRef](#)]
27. Wang, K.K.; Graham, I.T.; Martin, L.; Voudouris, P.; Giuliani, G.; Lay, A.; Harris, S.J.; Fallick, A.E. Fingerprinting Paranesti Rubies through Oxygen Isotopes. *Minerals* **2019**, *9*, 14. [[CrossRef](#)]
28. Karampelas, S.; Kiefert, L. Gemstones and Minerals. In *Analytical Archaeometry*; Edwards, H., Vandenabeele, P., Eds.; The Royal Society of Chemistry: Cambridge, UK, 2012; pp. 291–317.
29. Groat, L.A.; Giuliani, G.; Stone-Sundberg, J.; Sun, Z.; Renfro, N.D.; Palke, A.C. A review of analytical methods used in geographic origin determination of gemstones. *Gems Gemol.* **2019**, *55*, 512–535. [[CrossRef](#)]
30. Beran, A.; Rossman, G.R. OH in naturally occurring corundum. *Eur. J. Mineral.* **2006**, *18*, 441–447. [[CrossRef](#)]
31. Balan, E. Theoretical infrared spectra of OH defects in corundum (α -Al₂O₃). *Eur. J. Mineral.* **2020**, *32*, 457–467. [[CrossRef](#)]

32. Smith, C.P.; Hartley, A.; Zelligui, R. Titanite (sphene) inclusions in ruby identified by infrared spectroscopy. *J. Gemmol.* **2020**, *37*, 11–12. [[CrossRef](#)]
33. Smith, C.P.; Zelligui, R. Vesuvianite (idiocrase) and apatite inclusions in ruby identifiable by infrared spectroscopy. *J. Gemmol.* **2020**, *37*, 346–348. [[CrossRef](#)]
34. Smith, C.P. A contribution to understanding the infrared spectra of rubies from Mong Hsu, Myanmar. *J. Gemmol.* **1995**, *24*, 321–335. [[CrossRef](#)]
35. Besson, G.; Drifts, V.A. Refined relationships between chemical composition of dioctahedral fine-grained mica minerals and their infrared spectra within the OH stretching region. Part I: Identification of the OH stretching bands. *Clays Clay Miner.* **1997**, *45*, 158–169. [[CrossRef](#)]
36. Phan, T.M.D. Internal Characteristics, Chemical Compounds and Spectroscopy of Sapphire as Single Crystals. Ph.D. Thesis, Johannes Gutenberg-Universität, Mainz, Germany, 2015; p. 140.
37. McClure, D.S. Optical spectra of transition-metal ions in corundum. *J. Chem. Phys.* **1962**, *36*, 2757–2779. [[CrossRef](#)]
38. Ferguson, J.; Fielding, P.E. The origins of the colours of natural yellow, green, and blue sapphires. *Chem. Phys. Lett.* **1971**, *10*, 262–265. [[CrossRef](#)]
39. Krebs, J.J.; Maisch, W.G. Exchange effects in the optical absorption spectrum of Fe^{3+} in Al_2O_3 . *Phys. Rev. B* **1971**, *4*, 757–769. [[CrossRef](#)]
40. Eigenmann, K.; Kunz, K.; Gunthard, H. The optical spectrum of $\alpha\text{-Al}_2\text{O}_3\text{:Fe}^{3+}$. *Chem. Phys. Lett.* **1972**, *13*, 54–57. [[CrossRef](#)]
41. Schmetzer, K. Zur Deutung der Farbursache blauer Saphire—Eine Diskussion. *Neues Jahrb. Fur. Mineral. Mon.* **1987**, *8*, 337–343.
42. Fritsch, E.; Rossman, G.R. An update on color in Gems Part II. Colors involving multiple atoms and color centers. *Gems Gemol.* **1988**, *24*, 3–15. [[CrossRef](#)]
43. Townsend, M.G. Visible charge transfer band in blue sapphire. *Solid State Commun.* **1968**, *6*, 81–83. [[CrossRef](#)]
44. Mattson, S.M.; Rossman, G.R. $\text{Fe}^{2+}\text{-Ti}^{4+}$ charge transfer in stoichiometric $\text{Fe}^{2+}\text{,Ti}^{4+}$ -minerals. *Phys. Chem. Miner.* **1988**, *16*, 78–82. [[CrossRef](#)]
45. Moon, A.R.; Phillips, M.R. Defect clustering and color in $\text{Fe,Ti:a-Al}_2\text{O}_3$. *J. Am. Ceram. Soc.* **1994**, *77*, 356–357. [[CrossRef](#)]
46. Fritsch, E.; Rondeau, B.; Devouard, B.; Pinsault, L.; Latouche, C. Why are some crystals gem quality? Crystal growth considerations on the “gem factor”. *Can. Mineral.* **2017**, *55*, 521–533. [[CrossRef](#)]
47. Liati, A.; Seidel, E. Metamorphic evolution and geochemistry of kyanite eclogites in central Rhodope, Northern Greece. *Contrib. Mineral. Petrol.* **1996**, *123*, 293–307. [[CrossRef](#)]
48. White, J.S. Boehmite exsolution in corundum. *Am. Mineral.* **1979**, *64*, 485–491.
49. Haas, H. Diaspore-corundum equilibria determined by epitaxis of diaspore on corundum. *Am. Mineral.* **1972**, *57*, 1375–1385.
50. Hänni, H. Origin determination of gemstones: Possibilities, restrictions and reliability. *J. Gemmol.* **1994**, *24*, 139–148. [[CrossRef](#)]
51. Smith, C.P. Inside sapphires. *Rapp. Mag.* **2010**, *33*, 123–132.
52. Smith, G. Evidence for absorption by exchange-coupled $\text{Fe}^{2+}\text{-Fe}^{3+}$ pairs in the near infrared spectra of minerals. *Phys. Chem. Miner.* **1978**, *3*, 375–383. [[CrossRef](#)]